

Improving transmission performance of optical resonator by thermal oxidation

Li Minghui^{1,2} Luo Liang^{1,2} Ma Kezhen^{1,2} Qiu Haitao^{1,2} Xue Chenyang^{1,2}
Zhang Wendong^{1,2} Yan Shubin^{1,2}

¹Key Laboratory of Instrumentation Science and Dynamic Measurement of Ministry of Education,
North University of China, Taiyuan, Shanxi 030051, China

²Science and Technology on Electronic Test & Measurement Laboratory, North University of China,
Taiyuan, Shanxi 030051, China

Abstract For improving the larger sidewall roughness of an optical waveguide and exploring the advantages of fractionated oxidation over a single oxidation process, silicon-on-insulator ring and racetrack cavities are prepared using microelectro-mechanical system (MEMS) technology. The silicon-on-insulator ring and racetrack cavities are optimized by single and double oxidation processes, respectively. The relationships among the roughness, scattering loss, and transmission characteristics of an optical resonator are theoretically analyzed and simulated. The experimental results show that, a narrower full-width at half-maximum (FWHM), higher quality factor (Q), and lower transmission loss are achieved by the double oxidation process, compared with those achieved by the single oxidation process, for the same oxidation thickness. This result provides a reference for surface-smoothing research and has a significant influence on the preparation and application of cavities with high Q and low transmission loss in filters, biosensors, optical gyroscopes, and other related fields.

Key words integrated optics; optical resonator; coupling experiment; oxidation; quality factor

OCIS codes 130.3120; 230.7370; 230.5750; 120.6660

热氧化法改善光学谐振腔的传输特性

李明慧^{1,2} 骆亮^{1,2} 马可贞^{1,2} 仇海涛^{1,2} 薛晨阳^{1,2} 张文栋^{1,2} 闫树斌^{1,2}

¹中北大学仪器科学与动态测试教育部重点实验室, 山西 太原 030051

²中北大学电子测试技术国家重点实验室, 山西 太原 030051

摘要 为了改善光学波导较大的侧壁粗糙度, 探究分次氧化工艺相比于单次氧化工艺的优势, 运用微机电系统 (MEMS) 工艺制备了绝缘体上硅环型谐振腔和跑道型谐振腔, 并通过单次氧化工艺和二次氧化工艺对其进行优化处理。理论分析并仿真了粗糙度、散射损耗和光学谐振腔传输特性之间的关系。实验结果显示, 相同的氧化深度下, 相比单次氧化工艺, 二次氧化工艺获得了较窄的半峰全宽 (FWHM)、较高的品质因数 (Q) 和较低的传输损耗。研究结果为波导表面光滑研究提供了重要的参考依据, 同时对于高 Q 值、低损耗谐振腔的制备及其在滤波器、生物传感和光学陀螺等相关领域中的应用具有重要的研究意义。

关键词 集成光学; 光学谐振腔; 耦合实验; 氧化; 品质因数

中图分类号 TN256 文献标识码 A

doi: 10.3788/CJL201542.0508005

收稿日期: 2014-11-06; 收到修改稿日期: 2015-01-07

基金项目: 国家自然科学基金重大研究专项(91123036)、国家自然科学基金面上项目(61178058, 61275166)、山西省高等学校中青年拔尖创新人才项目、中北大学杰出青年基金支持计划

作者简介: 李明慧(1988—), 女, 硕士研究生, 主要从事微纳器件光波导与系统集成方面的研究。

E-mail: liminghui1207@163.com

导师简介: 闫树斌(1975—), 男, 博士, 副教授, 主要从事光学微腔, 集成光学传感方面的研究。

E-mail: shubin_yan@nuc.edu.cn(通信联系人)

1 Introduction

Optical resonators based on silicon-on-insulator (SOI) technology have been more attractive in fields of optical filters^[1-2], modulators^[3], all-optical switching devices^[4], and optical gyroscopes^[5-6], owing to their advantages of low fabrication cost, high integration, and compatibility with complementary-metal-oxide-semiconductor (CMOS) technology^[7]. However, optical resonators commonly have larger sidewall roughness induced during the etching process, which prevents the realization of high quality factor (Q) and ultra-low loss. At present, some research institutions have carried out many studies to reduce the roughness down to the nanometer level, using approaches such as hydrogen annealing and excimer laser reformation. From research conducted domestically and globally, hydrogen annealing changes the basic shape of the structure and hydrogen gas determines a certain risk in actual operation; on the other hand, there are too many experimental parameters to be controlled in laser reformation, and the structure may easily be subjected to damage if any of the parameters is not set properly. Except for these limitations, these studies are mostly restricted to reduce the roughness and loss coefficient^[8-10], and only few studies focus on the overall improvement in transmission performance, which includes improving the full-width at half-maximum (FWHM) and quality factor in optical cavities after roughness reduction.

Surface treatment is proposed using fractionated oxidation based on the traditional single oxidation process. Theoretical analysis and simulation are performed to completely understand the relationships among roughness, transmission loss, and quality factor. Ring and racetrack resonators based on SOI technology are fabricated using microelectro-mechanical system (MEMS) technology. Then, the single and double oxidation processes are optimized for each resonator with good consistency. The experimental results show that the cavities optimized through double oxidation have a narrower FWHM, higher- Q value, and lower transmission loss than those optimized through the single oxidation process, for the same oxide thickness. The findings provide a reference for parameter setting in thermal oxidation, and also offer support for research on surface-smoothing of optical waveguides.

2 Theory

Losses in sub-micron waveguides include absorption loss, scattering loss, radiation loss, and bending loss. Scattering loss, induced by sidewall roughness, constitutes a major part of these losses. Generally, the sidewall of a waveguide prepared by lithography and etching processes is rougher than the top surface. The Payne-Lacey theory^[11-12] gives the scattering loss per unit length, induced by roughness, as follows:

$$\alpha = 4.34 \frac{\sigma^2}{\sqrt{2} \kappa W^4 N_{\text{clad}}} g(V) \cdot \xi(\chi, \gamma), \quad (1)$$

where σ is the root-mean-square (RMS) roughness, κ is the free-space wavenumber, W and N_{clad} represent the waveguide width and cladding refractive index, respectively, and $g(V)$ and $\xi(\chi, \gamma)$ are the slowly varying functions of various parameters in the waveguide, which can be ignored as their effect on the loss is negligible. It follows that the width and RMS roughness are the main impact factors. Figure 1(a) shows the relationship between the scattering loss and RMS roughness for different widths. Furthermore, the simulation is represented in Fig. 1(b) using the transfer matrix method^[13], to study the influences of different transmission loss coefficients on the resonance characteristics of the resonator (radius is 20 μm).

It can be observed that the scattering loss coefficient increases with the increase in RMS roughness and changes drastically when the waveguide width is smaller [see Fig. 1(a)]. For a RMS roughness larger than 20 nm, the scattering loss coefficient is nearly 100 dB/cm for a waveguide with a 350 nm width; this is a critical issue in optical transmission. In addition, a higher loss leads to a shallower resonant depth and broader FWHM, as shown in Fig. 1 (b), which results in a lower quality factor. As a result, the scattering loss induced by the roughness cannot be neglected. Reducing the roughness of the waveguide to realize a smoother surface, higher- Q value, and lower

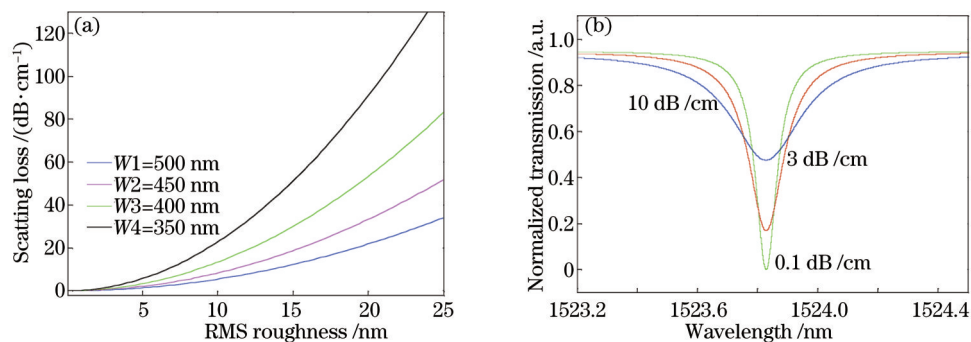


Fig.1 (a) Relationship between RMS roughness and scattering loss for different widths; (b) resonance curves of ring-resonator with different scattering loss coefficients

loss, is essential for the development and application of micro-nano devices.

3 Process and test

3.1 Preparation and optimization

Silicon-on-insulator is the material commonly used in fabricating optical cavities for its excellent ability to restrict the optical field owing to the larger refraction difference between Si and SiO₂ layers^[14]. Ring cavities (radius is 20 μm) and racetrack resonators (circumference is 331.42 μm) are prepared by MEMS technology. Scanning electron microscopes of the resonators are shown in Fig.2.

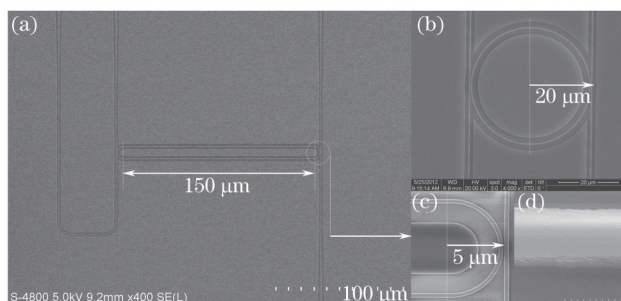


Fig.2 Scanning-electron-microscopes. (a) Racetrack resonator; (b) ring resonator; (c) partial enlarged detail of racetrack resonator; (d) sidewall roughness

Compared with other surface-smoothing processes, thermal oxidation is relatively easier to perform with a more simple principle, and the more obvious protrusions on silicon surface own the faster reaction rate of oxidation under a certain oxidation depth. Therefore, the silicon consumed during the process is almost the roughness in surface and sidewall, and the oxidation process retains the basic shape of the structure. The schematic diagram of the oxidation and temperature curve is shown in Fig.3. Eventually, we obtain a smoother surface after the removal of the oxide layer by wet corrosion.

Before the resonators are put into the oxidizing furnace, it should be ensured that they do not have any metal impurities. As shown in Fig.3, the furnace is initially heated to 300 °C. Then, it is heated for 2 h (t_1) at a rate of 5 °C/min until it reaches the desired reaction temperature (900 °C). Then, oxygen is passed into the furnace at a rate of 6 L/min for time t_2 , and it generally requires more than 3 h (t_3) for cooling. A sufficient amount of nitrogen is supplied in both heating and cooling stages in order to ensure that the samples cannot be polluted by other gaseous ingredients in the air.

One group of structures is fabricated by single oxidation for 33 min (t_2), and the others group is fabricated by the double oxidation process, and t_2 is followed by 8.5 min and 4.5 min (the oxide layer has to be removed between the two processes). An ellipsometry test is carried out after each oxidation process to measure the oxide thickness on the surface; the results show that the thickness of the oxide layer after single oxidation is 15.495 nm, and after double oxidation is

9.165 nm and 6.214 nm respectively, which can be approximated as the same oxidation depth as the result in the single oxidation process. We use the buffered-oxide-etch (BOE, $V_{HF}:V_{NH_4F}=1:20$) solution to remove the oxide layer after calibrating the rate of corrosion and controlling the corresponding corrosion time accurately.

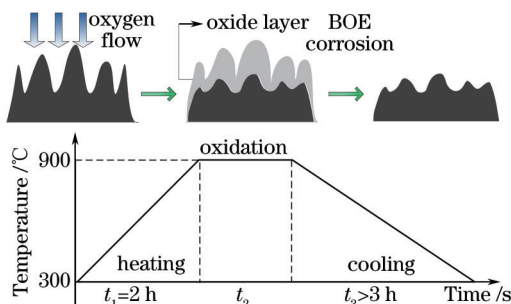


Fig.3 Schematic diagram of oxidation and temperature curve

3.2 Coupling experiment

The structures (before oxidation, after single oxidation, and after double oxidation) are tested in the same coupling experimental system. The coupling principle diagram is represented in Fig.4.

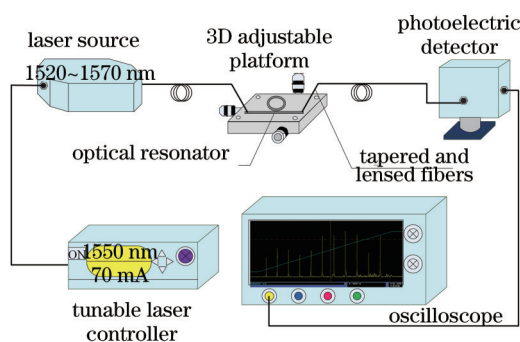


Fig.4 Coupling principle diagram

A tunable laser, which has a scan range from 1520 nm to 1570 nm, is used as the laser source. The optical resonators are placed on the three-dimensional (3D) adjustable platform. We adjust the tapered and lensed fibers both in the input and output of the optical resonator to achieve the best coupling state. The signals that pass through the photoelectric detector are obtained on the oscilloscope, and then, we obtain the transmission spectra of the optical cavities.

4 Results and analysis

Using the data from the results of the coupling experiment, transmission lines in a certain range of wavelength are represented in Figs.5(a) and (b).

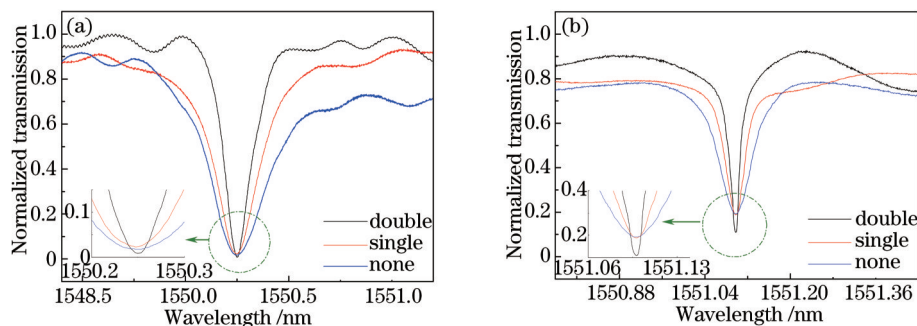


Fig.5 Contrast of normalized transmission lines before and after oxidation optimization. (a) Resonance spectra of ring microcavity; (b) resonance spectra of racetrack microcavity

It can be observed that the FWHM becomes significantly narrower after optimization irrespective of whether it is a ring or racetrack microcavity, and the narrowest FWHM and highest- Q value are achieved especially after the double oxidation process. The smooth surface reduces the scattering loss, and the coupling gap between the resonator and the channel waveguide becomes larger after BOE corrosion, thus decreasing the coupling coefficient and further obtaining a narrower FWHM. The FWHM values of the ring resonator before oxidation, after single oxidation, and after double oxidation, are 0.32, 0.25, and 0.15 nm, corresponding to Q_{loaded} values of ~ 4845 , ~ 6201 , and ~ 10340 , respectively; the FWHM values of the racetrack resonator are respectively 0.075, 0.045, and 0.025 nm, corresponding to Q_{loaded} values of ~ 20680 , ~ 34470 , and ~ 62040 , achieving a significant improvement over the values for the ring resonator.

The scanning electron microscope images of the surface on the waveguide are captured after single and double oxidation processes, as shown in Figs.6(a) and (b).

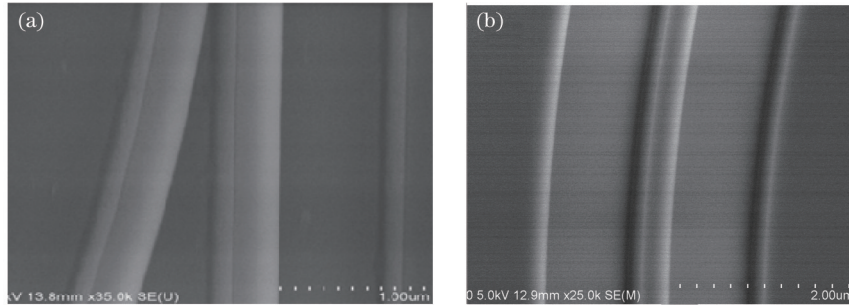


Fig.6 Scanning electron microscope images. (a) After single oxidation; (b) after double oxidation

It seems that both single and double oxidations achieve a smoother surface compared with the surface illustrated in Fig.2(d), and in particular, the double oxidation process achieves a more desired effect. However, because of the difficulty in measuring sidewall roughness, the reduction extent of sidewall roughness can be characterized by the variation in the scattering loss coefficient. Relationship between the intrinsic quality factor Q_{int} and the scattering loss coefficient in the waveguide resonator^[15-17] is shown as

$$Q_{\text{int}} = \frac{2Q_{\text{loaded}}}{1 + \sqrt{T_0}}, \quad (2)$$

$$\alpha = \frac{2\pi N_g}{\lambda_0 Q_{\text{int}}} = \frac{\lambda_0}{Q_{\text{int}} \cdot F_{\text{FSR}} \cdot R}, \quad (3)$$

where T_0 is the normalized transmission energy at the resonance point λ_0 ; N_g , F_{FSR} , and R are the group index, free spectral width, and radius, respectively. The scattering loss coefficients calculated before and after the oxidation optimization are listed in Table 1.

Table 1 Scattering loss coefficients

Optical cavity	Before oxidation /(dB/cm)	Single oxidation /(dB/cm)	Double oxidation /(dB/cm)
Ring-type	1.327	1.242	1.014
Racetrack-type	0.792	0.598	0.313

Indeed, the double oxidation process achieves a smoother surface and lower transmission loss under the same oxidation thickness, thus creating a higher quality factor, which is consistent with the theoretical simulation presented in the theory section. The research results indicate that oxidation depth is not proportional to reaction time; thus, the oxide layer generated initially prevents further oxidation of the roughened surface of the structure. Therefore, the reactive time required in the double oxidation process is theoretically less than that required in the single oxidation process for the same oxide thickness. Further, the waveguide surface after wet corrosion is more smoother, achieving a reduced transmission loss.

Because it is difficult to achieve a higher quality factor for optical cavities owing to larger roughness, this study

summarizes a conjecture that, if the relationships between the parameters of the oxidation process and the oxide depth can be controlled accurately, performing oxidation more than two times can enable fabricating resonators with a smoother surface, larger size, and higher- Q value.

5 Conclusion

A better method for fractionated oxidation to improve the large sidewall roughness of optical cavities caused by MEMS processes is proposed. The experimental results show that the double oxidation process has a conspicuous advantage of obtaining narrower FWHM, higher- Q value, lower transmission loss, and an overall deeper resonance spectrum compared with that of single oxidation process under the same oxidation depth. The findings of our study enable surface optimization of optical waveguides and help achieve microcavities with a larger size and higher- Q value. This contributes to the development and application of optical resonators in the fields of filters, wavelength division multiplexers, and in particular, optical gyroscopes.

Acknowledgements

The authors thank the Suzhou Institute of Nano-Tech and Nano-Bionics of the Chinese Academy of Sciences for contribution to the fabrication of the devices.

References

- 1 P Zou, X Y Han, Y Wang, *et al.*. Study on a tunable radio frequency filter based on integrated optical waveguide[J]. *Acta Optica Sinica*, 2013, 33(10): 1013001.
邹品, 韩秀友, 王瑜, 等. 可调谐集成光波导射频滤波器研究[J]. *光学学报*, 2013, 33(10): 1013001.
- 2 J Yang, S Xu, K Zhou, *et al.*. High performance and compact 1×3 beam splitter based on parallel silicon waveguide[J]. *Chin Opt Lett*, 2014, 12: S10501.
- 3 Y Ren, M P Song. Optical NRZ-to-RZ modulation format conversion based on cross-phase modulation effects in silicon micro-ring resonator[J]. *Acta Optica Sinica*, 2013, 33(7): 0706002.
任艳, 宋牟平. 基于硅基微环谐振器交叉相位调制效应的非归零信号到归零信号光调制格式转换[J]. *光学学报*, 2013, 33(7): 0706002.
- 4 Y Liu, X G Tong, J L Yu, *et al.*. All-optical switching in silicon-on-insulator serially coupled double-ring resonator based on thermal nonlinear effect[J]. *Chinese J Lasers*, 2013, 40(2): 0205006.
刘毅, 仝晓刚, 于晋龙, 等. 基于热非线性效应的硅基串联双微环谐振腔全光开关[J]. *中国激光*, 2013, 40(2): 0205006.
- 5 J R E Toland, C P Search. Sagnac gyroscope using a two-dimensional array of coupled optical microresonators[J]. *Appl Phys B*, 2014, 114(3): 333-339.
- 6 H Mao, H Ma, Z Jin. Polarization maintaining silica waveguide resonator optic gyro using double phase modulation technique[J]. *Opt Express*, 2011, 19(5): 4632-4643.
- 7 X Wang, J Chen, Y Dong, *et al.*. Formation of ultra-thin silicon-on-insulator materials by low-dose low-energy oxygen ion implantation[J]. *Chem Phys Lett*, 2003, 367(1): 44-48.
- 8 E Liang, S Hung, Y P Hsieh, *et al.*. Effective energy densities in KrF excimer laser reformation as a sidewall smoothing technique[J]. *J Vac Sci Technol B*, 2008, 26(1): 110-116.
- 9 M C M Lee, M C Wu. Thermal annealing in hydrogen for 3-D profile transformation on silicon-on-insulator and sidewall roughness reduction[J]. *J Microelectromechanical Systems*, 2006, 15(2): 338-343.
- 10 Q Xia, P F Murphy, H Gao, *et al.*. Ultrafast and selective reduction of sidewall roughness in silicon waveguides using self-perfection by liquefaction[J]. *Nanotechnology*, 2009, 20(34): 345302.
- 11 F P Payne, J P R Lacey. A theoretical analysis of scattering loss from planar optical waveguides[J]. *Opt Quant Electron*, 1994, 26(10): 977-986.
- 12 K O Latunde-Dada, F P Payne. Impact of waveguide sidewall roughness on the output uniformity and phase of MMI splitters[J]. *Opt Quant Electron*, 2008, 40(11-12): 863-873.
- 13 I Kiyat, C Kocabas, A Aydinli. Integrated micro ring resonator displacement sensor for scanning probe microscopies[J]. *J Micromech Microeng*, 2004, 14(3): 374-381.
- 14 C Qiu, Z Sheng, L Li, *et al.*. High efficiency grating couplers based on shared process with CMOS MOSFETs[J]. *Chin Phys B*, 2013, 22(2): 024212.

- 15 P E Barclay, K Srinivasan, O Painter. Nonlinear response of silicon photonic crystal microresonators excited via an integrated waveguide and fiber taper[J]. Opt Express, 2005, 13(3): 801-820.
- 16 L W Luo, G S Wiederhecker, J Cardenas, *et al.*. High quality factor etchless silicon photonic ring resonators[J]. Opt Express, 2011, 19(7): 6284-6289.
- 17 A Griffith, J Cardenas, C Poitras, *et al.*. High quality factor and high confinement silicon resonators using etchless process[J]. Opt Express, 2012, 20(19): 21341-21345.

栏目编辑: 张 雁